

Interfacing Unstructured Tetrahedron Grids to Structured-Grid FDTD

Douglas J. Riley and C. David Turner, *Member, IEEE*

Abstract—Finite-element unstructured tetrahedron grids provide considerable modeling flexibility but can give rise to an extremely large number of cells when solving open-region problems. The finite-volume hybrid-grid (FVHG) algorithm enables unstructured grids to be combined with traditional structured-grid, rectangular-cell, finite-difference time-domain (FDTD), thereby considerably reducing the unstructured-mesh overhead in surrounding space. In this letter, a simple technique to interface free-meshed, tetrahedron grids with FDTD is described. The two grids are directly coupled without the need for spatial interpolation. The tetrahedron mesh is defined to terminate on a rectangular surface that may be located very close to the geometry under study. Absorbing boundary conditions are easily applied in the surrounding FDTD grid. This technique provides finite-element modeling flexibility with the benefits of explicit time differencing and limited unstructured-mesh overhead. Multimaterial regions can be solved. The FVHG algorithm has been found to be accurate and generally stable for the long-term, even with complex free meshes generated by advanced solid-modeling software.

I. INTRODUCTION

TRADITIONAL FDTD is an efficient solution method, but it can provide only a “stair-case” approximation to curvature. This approximation can lead to considerable computational error [1] if the number of cells-per-wavelength is not increased. Because of this, there is interest in the development of accurate and efficient body-conforming, volumetric Maxwell solvers. Transient solvers based on computational fluid dynamics (CFD) techniques [2], finite-volumes [3]–[6], and local contour modifications [7] are under development. Finite-element approaches, although primarily used in the frequency domain, are also receiving attention in the time domain [8]. The accuracy and efficiency associated with various nonorthogonal cell shapes is of considerable importance with all methods, and late-time stability becomes an additional concern with transient approaches. Some algorithms, such as the CFD-based formulation, advance both the electric and magnetic fields on a single grid, whereas the approaches described [3]–[7] use two offset grids typically referred to as primary and dual grids.

Much of the previous work on transient nonorthogonal algorithms is based on grids generated by mapped-meshing techniques. Such grids are generally composed of hexahedral-and/or wedge-shaped cells and are block structured, although the grids can be referenced using unstructured techniques.

Manuscript received February 9, 1995. This work was supported by the U.S. Department of Energy under Contract DE-AC04-94AL85000.

The authors are with the Radiation and Electromagnetic Analysis Department, Sandia National Laboratories, Albuquerque, NM 87185-1166 USA.

IEEE Log Number 9413483.

Mapped-meshing usually requires partitioning the geometry to construct the mesh and is therefore not as flexible as free-meshing algorithms. Free meshing generally gives rise to fully unstructured tetrahedron grids, although free-meshing hexahedral algorithms are presently being developed [9]. Mapped-mesh grids provide a more visually satisfying mesh than grids obtained from free-meshing, but the overall quality of the grid with regard to cell stretch and distortion is often superior with tetrahedral elements.

This letter discusses free-meshing with linear tetrahedrons when used in conjunction with the finite-volume hybrid-grid (FVHG) technique [5]. The finite-volume portion of the FVHG solver uses a generalization/simplification of the modified finite-volume algorithm introduced in [3] and adds a time-averaging scheme to obtain late-time stability on complex grids. For open-region problems, the FVHG algorithm embeds an unstructured grid in a traditional FDTD code. Either an analytic or a Berenger-type [10] absorbing boundary condition is easily applied in the structured grid without incurring considerable overhead. The unstructured region is designed to terminate so that a direct connection to the structured grid occurs without spatial interpolation between grids. A transition from unstructured tetrahedrons to structured-grid FDTD has been accomplished within a minimum of 1–2 finite elements from solid models generated by I-DEAS [11]. This distance is remarkably close to the solid model and has lead to highly resolved grids without an excessive number of nonorthogonal cells. The direct connection of these tetrahedrons to the cubical hexahedrons used by the FDTD method is discussed below.

II. UNSTRUCTURED/STRUCTURED MESH INTERFACE

An I-DEAS generated tetrahedron grid of a sphere embedded in a closely spaced cubical box with the proper unstructured-grid termination characteristics is shown in Fig. 1. The surface of the bounding box was partitioned into quadrilateral sub-surfaces such that the nodes at the vertices of these surfaces will spatially align with the nodes of the structured FDTD grid that will ultimately be connected. The creation of the proper surface partitions can be accomplished easily within I-DEAS. When the tetrahedron grid terminates on this partitioned box the surface quadrilaterals become split into two isosceles triangles. To connect an FDTD cubical grid requires a simple transition layer called the “wrapper.” The wrapper is generated automatically during the pre-processing phase by analyzing the termination structure of the tetrahedron grid.

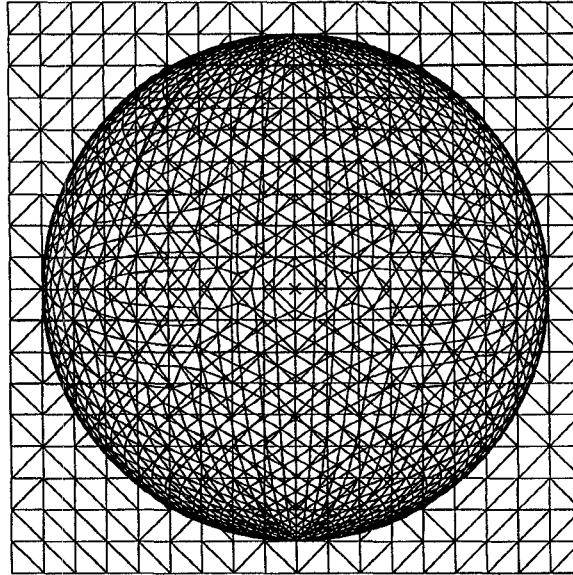


Fig. 1. Tetrahedron grid of a sphere embedded in a cubical box. On the six faces of the bounding box the bases of the tetrahedral elements exhibit an isosceles triangular form that will enable the direct connection of a structured FDTD grid. The FDTD grid fills the remainder of the problem space.

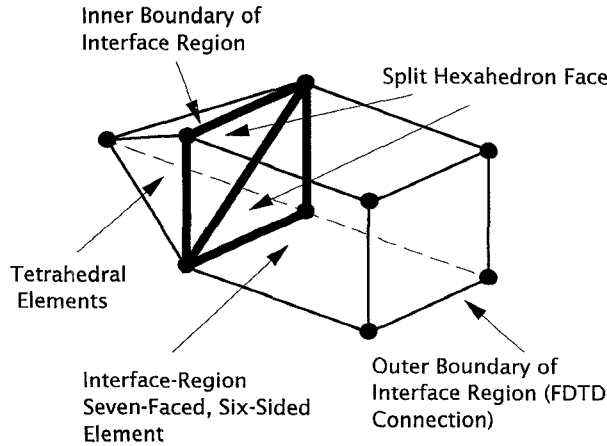


Fig. 2. Creation of a seven-face, six-sided element to interface unstructured tetrahedrons with structured FDTD elements.

A hexahedral element interfaced to the bases of two tetrahedral cells is shown in Fig. 2. For use with the FVHG algorithm, one face of this hexahedron is split into two isosceles triangles; this cell is treated as a seven-faced element. A layer of these special hexahedral cells is wrapped completely around the unstructured grid. The tetrahedron grid terminates on the *inner boundary* of the wrapper while the FDTD grid connects to the *outer boundary*. Standard cubical FDTD cells interface directly to the special hexahedral elements without spatial interpolation; this enables simple FDTD cells to be used to fill the remainder of the computational volume out to the termination of the grid. To increase the accuracy and dynamic range of the simulation, the code is run in scattered-field mode. This eliminates any numerical reflections the incident field may encounter when hitting the tetrahedron interface.

The complete time-advancement scheme is as follows. The electric (**E**) fields in the structured grid are initially ad-

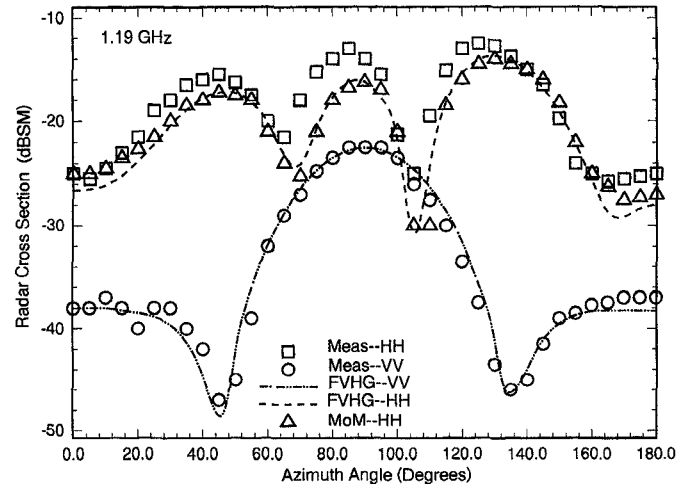


Fig. 3. Monostatic RCS for the 9.936-in. NASA metallic almond [12].

vanced. The FDTD **E**-fields on the outer boundary of the wrapper are second-order time-interpolated and mapped into the unstructured-grid registers. The unstructured region is advanced (possibly) several sub-time steps as dictated by the Courant condition in this region. The unstructured **E**-fields are subsequently mapped into the FDTD registers on the inner boundary of the wrapper. Advancing the FDTD magnetic (**H**) fields in the structured grid completes the overall time step.

III. NASA ALMOND

Geometry, measurements, and method-of-moment (MoM) calculations for the monostatic radar cross-section (RCS) of the 9.936-in. NASA almond were presented in [12]. The FVHG analysis of this geometry is presented here. The reader is referred to reference [12] for geometry details. A total of 65 000 tetrahedral elements were used to model the almond embedded in a closely spaced rectangular box; approximately 15 000 of these elements filled the almond's interior. Based on a maximum (taken over the primary and dual grids) average edge length, the unstructured grid provided 13 "cells" per wavelength at 3.5 GHz. This tetrahedron grid was embedded in a $68 \times 38 \times 68$ structured FDTD grid with second-order Mur absorbing boundaries. Attempting to fill this entire volume with tetrahedrons would have lead to millions of elements (it is noted that impedance-matched absorbing layers could be used with the tetrahedrons, but accuracy and efficiency has been found to be superior using the hybrid-grid approach).

The monostatic RCS at 1.19 GHz for the vertical/vertical (VV) and horizontal/horizontal (HH) cases [12] are shown in Fig. 3. Measured data are only provided at 5° intervals and were obtained by visually averaging the data displayed in [12]. Although the HH FVHG results differ from the measurements by 2–4 dBFSM (dB square m) for certain angles, the results are globally very close to the published MoM calculations [12].

IV. CONCLUDING REMARKS

The FVHG algorithm provides a seamless connection between unstructured and structured grids that is free from spatial interpolation across grid boundaries. A simple technique using

seven-faced, six-sided elements was introduced to directly connect finite-element-like tetrahedron grids with traditional structured-grid FDTD. By treating a nonorthogonal region as a local problem within a structured computational volume, computer resources are greatly reduced while adding full 3D solid-modeling flexibility without the geometrical limitations of mapped-meshing. Multimaterial regions are easily accommodated within the unstructured grid.

One of the most powerful applications of the FVHG technique is to geometries with extrusions, such as aircraft wings and tails. Highly absorbing boundaries must be sufficiently far removed so that interaction between the extrusions is not destroyed. Thus, a large amount of uninteresting space must be gridded. With the FVHG algorithm, this space is gridded with simple FDTD cells instead of costly tetrahedral elements.

Another application that is particularly well suited to the FVHG technique is microelectronics. This is because areas with high complexity can be modeled with tetrahedral elements while low complexity areas are modeled with FDTD. Coupling between regions occurs through the FVHG wrapper. However, care is required in the implementation because different cell types provide different impedances to propagating waves that can cause numerical reflections at interfaces. These reflections can often be suppressed by greater than 50 dB with minor adjustments to the material properties in each grid. Papers describing this application are forthcoming.

ACKNOWLEDGMENT

The authors thank Structural Dynamics Research Corporation (SDRC) for their assistance in adapting the I-DEAS

finite-element software to the mesh-termination requirements of the FVHG algorithm.

REFERENCES

- [1] R. Holland, "Pitfalls of staircase meshing," *IEEE Trans. Electromagn. Compat.*, vol. 35, no. 4, pp. 434-439, Nov. 1993.
- [2] V. Shankar, A. H. Mohammadian, and W. F. Hall, "A time-domain, finite-volume treatment for the Maxwell equations," *Electromagnetics*, vol. 10, no. 1-2, pp. 127-145, 1990.
- [3] N. K. Madsen and R. W. Ziolkowski, "A three-dimensional modified finite volume technique for Maxwell's equations," *Electromagnetics*, vol. 10, no. 1-2, pp. 147-161, 1990.
- [4] N. K. Madsen, "Divergence preserving discrete surface integral methods for Maxwell's curl equation using nonorthogonal unstructured grids," RIACS Tech. Rep. 92.04, NASA Ames Research Center, CA, Feb. 1992.
- [5] D. J. Riley and C. D. Turner, "Unstructured finite-volume modeling in computational electromagnetics," in *11th Annual Review of Progress in Applied Computational Electromagnetics (ACES) Symp. Dig.*, Mar. 1995, pp. 435-444.
- [6] K. S. Yee and J. S. Chen, "Conformal hybrid finite-difference time-domain (FDTD) with finite-volume time domain," *IEEE Trans. Antennas Propagat.*, vol. 42, no. 10, pp. 1450-1455, Oct. 1994.
- [7] T. G. Jurgens and A. Tafove, "Three-dimensional contour FDTD modeling from single and multiple bodies," *IEEE Trans. Antennas Propagat.*, vol. 41, no. 12, pp. 1703-1708, Dec. 1993.
- [8] J.-F. Lee, "Whitney elements time domain (WETD) methods for solving three-dimensional waveguide discontinuities," in *11th Annual Review of Progress in Applied Computational Electromagnetics (ACES) Symp. Dig.*, Mar. 1995, pp. 1258-1265.
- [9] CUBIT, Sandia National Laboratories, Albuquerque, NM, Dept. 1425, private communication, Mar. 1994.
- [10] J.-P. Berenger, "A perfectly matched layer for the absorption of electromagnetic waves," *J. Comp. Phys.*, vol. 114, pp. 185-200, 1994.
- [11] I-DEAS, Structural Dynamics Research Corporation, Milford, OH.
- [12] A. C. Woo, H. T. G. Wang, M. J. Schuh, and M. L. Sanders, "Benchmark radar targets for the validation of computational electromagnetics programs," *IEEE Antennas Propagat. Mag.*, vol. 35, no. 1, pp. 84-89, Feb. 1993.